

## Viscoelastic properties of amorphous polymers 3: low molecular weight poly(methylphenylsiloxane)\*)

D. J. Plazek<sup>1</sup>), C. A. Bero<sup>1</sup>), S. Neumeister<sup>1</sup>), G. Floudas<sup>2</sup>), G. Fytas<sup>2</sup>), and K. L. Ngai<sup>3</sup>)

<sup>1</sup>) Department of Materials Science and Engineering, University of Pittsburgh, Pittsburgh, Pennsylvania, USA

<sup>2</sup>) Foundation for Research and Technology-Hellas, Heraklion, Crete, Greece

<sup>3</sup>) Naval Research Laboratory, Washington, D.C., USA

\*) Dedicated to Prof. Dr. E. W. Fischer on his 65th Birthday. Prof. Dr. Fischer is known for his valuable contribution to fostering international collaboration of research in polymer science. This work is an example of his contribution because it would not be possible without him bringing us together. One of us (KLN) would like to take this opportunity to thank Prof. Dr. Fischer for his unwaiving support of the 1st (Crete) and the 2nd (Alicante) International Discussion Meeting on Relaxations in Complex Systems

**Abstract:** By making creep and recoverable creep measurements of a nearly monodisperse low molecular weight poly(methyl phenyl siloxane) sample, we have found on decreasing temperature towards  $T_g$  that there is continuously a change in the viscoelastic spectrum concomitant with a decrease of the steady-state recoverable compliance. This behavior is exactly the same as previously observed in low molecular weight poly(styrene), proving that this spectacular anomaly in the viscoelasticity of low molecular weight polymers is general and deserves an explanation. Photon correlation spectroscopic measurements performed on the same sample have extended the observation of the viscoelastic response to shorter times and the result corroborates the trend of variation established by the creep data.

**Key words:** Viscoelasticity – creep compliance – photon correlation spectroscopy – poly(methylphenylsiloxane)

### 1. Introduction

Most often it is assumed that all viscoelastic mechanisms observed above the glass temperature,  $T_g$ , are governed by the same temperature dependent friction coefficient,  $\zeta_0(T)$ . The entire viscoelastic spectrum shifts with temperature by an amount as determined by the shift factor

$$a_0(T) = [\zeta_0(T)/\zeta_0(T_0)], \quad (1)$$

where  $T_0$  is a reference temperature. This property has been called thermorheological simplicity [1]. This simplicity however usually does not hold. Precise experimental data in high molecular weight and entangled linear poly(styrene) (PS) [2–4] poly(vinylacetate) (PVAc) [5], amorphous poly(propylene) (a-PP) [6] and other polymers

[7–9] have shown beyond any doubt that the shift factor  $a_{T\eta}$  of the terminal dispersion is significantly smaller than that,  $a_{T\alpha}$ , of the segmental motion. This difference between  $a_{T\eta}$  and  $a_{T\alpha}$  has been explained by the coupling model [10, 11].

In several amorphous polymers of high molecular weight, Plazek et al. [12] have compared their recoverable compliances with dynamical shear compliance measurements of Williams, Fitzgerald, and Ferry [13] taken at higher frequencies/shorter times and higher temperatures. Comparison between the retardation spectra of these two sets of experimental data indicate that the retardation times of Rouse modes shift less with temperature than the segmental motion.

In low molecular weight unentangled PS, time-temperature equivalence of the recoverable creep

compliance,  $J_r(t)$ , was found to be invalid [14–17] also. In fact, the steady-state recoverable compliance,  $J_e^0$ , is a strong function of temperature. Far above  $T_g$ ,  $J_e^0$  attains a value which is close in magnitude to the predicted value from the Rouse model modified [1] for an undiluted polymer. As the temperature is decreased towards the glass temperature  $T_g$ ,  $J_e^0$  decrease continuously. The retardation spectra,  $L(\tau)$ , calculated from  $J_r(t)$  are not thermorheologically simple because at different temperatures the shape of  $L(\tau)$  changes. An explanation of this spectacular temperature dependence of  $J_e^0$  has been given also by the coupling model [14–17]. Although this dramatic viscoelastic property has been established experimentally beyond any doubt in low molecular weight polystyrenes [14, 15], it has not been studied in other low molecular weight amorphous polymers except poly(propyleneglycol) (PPG) [18]. In PPG, hydrogen bondings [19] between chains may complicate the Rouse chain dynamics and the situation may not be exactly equivalent to PS. It would be desirable to make viscoelastic measurements in another polymer that has no additional complications and confirm the general observation of this anomalous viscoelastic property in low molecular weight unentangled polymers.

Dynamic light-scattering experiments performed [16] some years ago on a poly(methylphenyl siloxane) PMPS with a weight average molecular weight,  $M_w$ , of 2500 have led us to the finding that the relaxation time,  $\tau_1$ , of the  $p = 0$  Rouse mode responsible for center-of-mass diffusion and the local segmental relaxation time,  $\tau_\alpha^*$ , have very different temperature and pressure,  $P$ , dependences. In fact, when data were fitted to the Vogel–Fulcher–Tamann–Hesse form

$$\tau_1 = \tau_s \exp[(B_1 + a_1 P)/R(T - T_0)] \quad (2)$$

and

$$\tau_\alpha^* = \tau_f \exp[(B_2 + a_2 P)/R(T - T_0)] \quad (3)$$

with the same  $T_0$ , the parameters  $B_2$  and  $a_2$  for the segmental motion are larger than the corresponding  $B_1$  and  $a_1$  for the  $p = 0$  Rouse mode by a factor approximately equal to 2. Actually  $B_1/R = 732 \pm 18$  K,  $a_1 = 32.4 \pm 0.8$  cm<sup>2</sup>/mol,  $B_2/R = 1659 \pm 43$  K,  $a_2 = 67.6 \pm 1.5$  cm<sup>3</sup>/mol, and  $T_0 = 207$  K [16]. These results from dynamic light scattering indicate that

$\tau_1$  and  $\tau_\alpha^*$  have different temperature and pressure shift factors and hence there is a breakdown of thermorheological simplicity. Thus, viscoelastic measurements on a low molecular weight PMPS should reveal whether the PS behavior is likely to be general or not.

In this work we present shear creep and recoverable creep compliance measurements on a nearly monodisperse sample of PMPS with a molecular weight of 5000. Photon correlation spectroscopy measurements were made in the same sample to extend the temperature range and time window of the creep measurements. The results to be reported in the following sections exhibit the same anomalous viscoelastic behavior as seen before in low molecular weight PS, and can be explained by the coupling model in the same manner as done previously [14–17].

## II. Creep and recoverable compliance measurements

### a. Experimental section

The isothermal creep,  $J(t)$ , and recoverable creep compliance,  $J_r(t)$ , measurements were carried out in a frictionless magnetic bearing torsional creep apparatus. The design and operation of the apparatus have been described earlier [2]. The PMPS sample was generously provided by

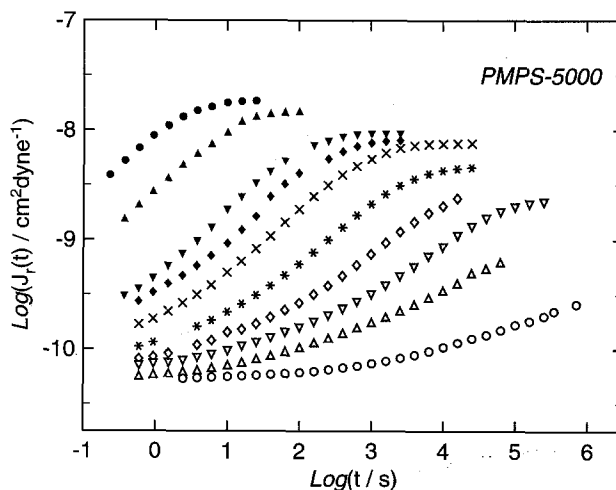


Fig. 1. Recoverable compliance,  $J_r(t)$ , of PMPS-5000 measured as a function of time for 10 different temperatures:  $-32.2^\circ$ ,  $-35.0^\circ$ ,  $-38.6^\circ$ ,  $-40.0^\circ$ ,  $-41.1^\circ$ ,  $-42.6^\circ$ ,  $-44.5^\circ$ ,  $-45.2^\circ$ ,  $-46.9^\circ$ ,  $-50.0^\circ$  C in order of decreasing  $J_r(t = 10$  s)

the Max Planck Institut für Polymerforschung-Mainz, Germany. The sample is nearly monodisperse and was reported to have a molecular weight of 5000. The glass temperature,  $T_g = -49.7^\circ\text{C}$ , was determined by monitoring the sample's length in the creep apparatus while it was cooled at  $0.3^\circ\text{C}/\text{min}$ . The recoverable creep compliance was measured at ten temperatures from  $-50$  to  $-32.2^\circ\text{C}$  and is presented in Fig. 1.

### b. Results and discussion

It can be seen from Fig. 1, the steady-state recoverable compliance  $J_e^0$  of PMPS decreases by a factor of about 60 times from the value of  $1.85 \times 10^{-8} \text{ cm}^2/\text{dyne}$  at the highest temperature  $-32.2^\circ\text{C}$  to the value of  $3.13 \times 10^{-10} \text{ cm}^2/\text{dyne}$  at the lowest temperature  $-50.0^\circ\text{C}$  of measurement (Fig. 2) This is comparable to the decrease of  $J_e^0$  by thirtyfold observed in 3400 molecular weight PS between  $100$  and  $70^\circ\text{C}$  [9, 10]. The features of the present data of PMPS are remarkably similar to that of PS. The data illustrated in Figs. 1 and 2 are sufficiently clear for us to conclude that the compliance measured in the range  $1.9 \times 10^{-8} > J_e^0 > 3.1 \times 10^{-10} \text{ cm}^2/\text{dyne}$  definitely comes from the Rouse modes and other modes that are intermediate in time and length scale between the local segmental mode and the Rouse modes. The recoverable compliance measurements (Fig. 1) have a time window of about six decades of time-scale, but it is still not wide

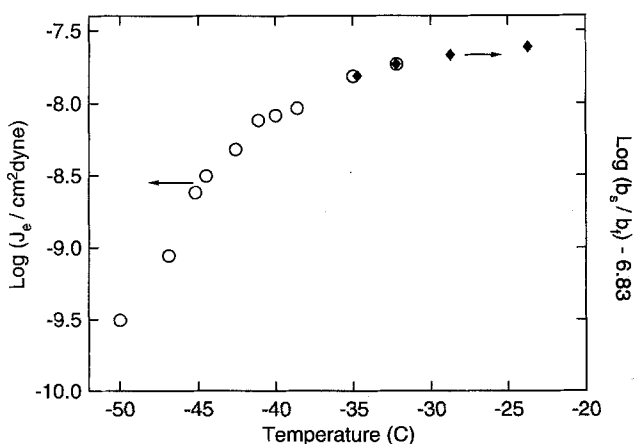


Fig. 2. Recoverable compliance  $J_e^0$ , obtained from creep measurements (open circles) plotted against temperature  $\text{Log}_{10}(b_s/b_r)$  obtained from photon correlation spectroscopy, shifted vertically downwards by 6.83 decades and plotted against temperature

Table 1. Shift factor,  $a_T$ , viscosity,  $\eta$ , and steady state recoverable compliance,  $J_e^0$ , of PMPS-5000 obtained from shear creep and recoverable creep compliance measurements.

Temp ( $^\circ\text{C}$ )	$\log a_T$	$\log \eta$ (Poise)	$\log J_e^0$ ( $\text{cm}^2/\text{dyne}$ )
23.4	—	1.472	—
9.35	—	1.997	—
-3.45	—	2.894	—
-19.2	—	4.672	—
-27.0	—	6.056	—
-32.2	-0.90	7.220	-7.733
-35.0	0.00	8.034	-7.815
-38.6	1.35	9.219	-8.035
-40.0	1.82	9.652	-8.085
-41.1	2.33	10.046	-8.118
-42.6	3.18	10.731	-8.320
-44.5	3.96	11.364	-8.505
-45.2	4.70	11.833	-8.620
-46.9	5.50	12.592	-9.056
-50.0	7.20	14.470	-9.505

enough to observe the local segmental motions and all the Rouse modes at a single temperature. The sets of isothermal data can be shifted horizontally to superpose on the rising shorter times side and form an asymptotic reduced curve (Fig. 3). The shift factors  $\log a_T$  used (Table 1) have a Vogel-Fulcher-Tammann-Hesse (VFTH) dependence of

$$\log a_T = A + B/(T - T_0), \quad (4)$$

where  $A = -20.39$ ,  $B = 1157.3$  and  $T_0 = -91.8^\circ\text{C}$ . This shift factor for the entire temperature range in which  $a_T$  is determined is neither entirely that of the segmental motion nor that of the Rouse modes. At  $-50^\circ\text{C}$  nearly all of the  $J_e(t)$  deformation is contributed by the segmental motions. Near this lowest temperature the shift factor is that of the local segmental motion. While near the highest temperature of  $-32.2^\circ\text{C}$ , this shift factor is that of the low mode number,  $p$ , Rouse modes. At intermediate temperatures it is clear that the shift factor describes the temperature dependence of neither of the local segmental relaxation nor the low  $p$  Rouse modes. This shift factor is obtained as a compromise between that of the segmental motions, the sub-Rouse modes, and the higher  $p$  Rouse modes. Above  $-42.6^\circ\text{C}$  the data points come entirely from sub-Rouse and Rouse modes throughout the experimental time window. The retardation spectra  $L(\log \tau)$  of PMPS - 5000 have been calculated numerically

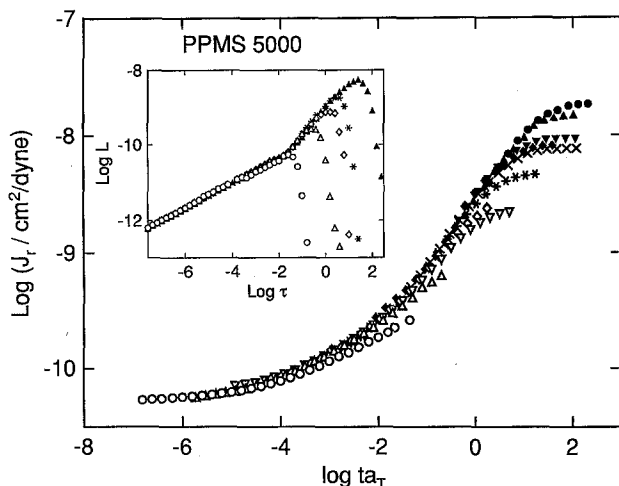


Fig. 3. Data of  $J_r(t)$  from Fig. 1 shifted to superpose at short times. Inset shows the retardation spectra of these shifted  $J_r$  data sets. Symbols same as used as Fig. 1

from the shifted  $J_r(t)$  data (Fig. 3) for several temperature of measurement via the relationship

$$J_r(t) = J_g + \int_{-\infty}^{\infty} L(\log \tau) (1 - e^{-t/\tau}) d \ln \tau, \quad (5)$$

where  $J_g$  is the glassy compliance and  $\tau$  is the retardation time. As seen previously in PS, the retardation spectrum (Fig. 3) shows a depletion of retardation mechanisms with decreasing temperature. The loss of mechanisms begins with Rouse modes having the longest retardation times. The explanation of the strong decrease of  $J_e$  and the depletion of retardation mechanism with decreasing  $T$  offered in refs. [15] and [17] for PS is applicable verbatim to PMPS.

A shift factor that truly represents only the segmental motions within the Rouse "submolecule" [1] can be obtained from Fig. 1 by restricting the consideration to data with  $J_r(t) < 10^{-9.7} \text{ cm}^2/\text{dyne}$ . To write down the contribution to recoverable compliance from segmental motions  $J_{ra}(t)$  we follow Read et al. [20], and Plazek et al. [21], and assume that  $J_{ra}(t)$  has the form

$$J_{ra}(t) = J_g + (J_{ea} - J_g)(1 - \exp -(t/\tau_\alpha^*)^{1-n_\alpha}), \quad (6)$$

where  $J_g$  is the glassy compliance,  $(J_{ea} - J_g)$  the total recoverable compliance contributed by the local segmental motions,  $n_\alpha$  is the coupling parameter, and  $\tau_\alpha^*$  the retardation time of the local segmental motion. We use Eq. (6) to fit first the recoverable creep compliance data taken at

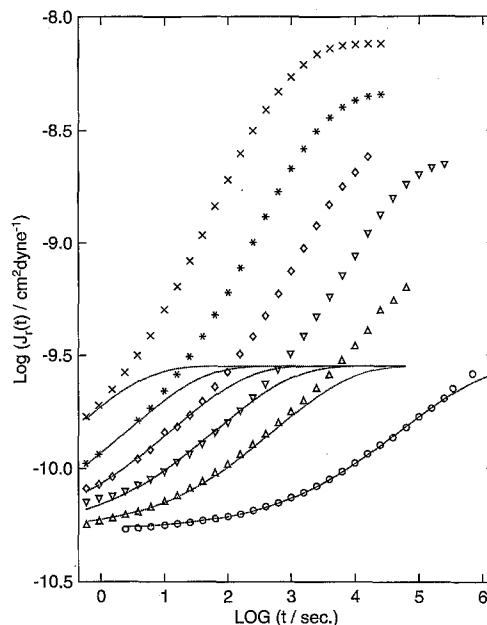


Fig. 4. Fits of the experimental data of  $J_r(t)$  to Eq. (6) (dotted curves) at six temperatures:  $-41.1$ ,  $-42.6$ ,  $-44.5$ ,  $-45.2$ ,  $-46.9$ ,  $-50.0$  °C in order of decreasing  $J_r(t = 10 \text{ s})$

the lowest temperature of  $-50$  °C. At this temperature, the data suggests that almost none of the Rouse modes contribute to the recoverable deformation and  $J_r(t)$  comes entirely from  $J_{ra}(t)$ . This fit shown in Fig. 4 determines  $J_{ea} = 2.82 \times 10^{-10} \text{ cm}^2/\text{dyne}$  and  $J_g = 5.39 \times 10^{-11} \text{ cm}^2/\text{dyne}$ . With  $J_{ea}$  and  $J_g$  fixed the curves in Fig. 4 are fits of  $J_{ra}(t)$  from Eq. 6 to the rest of the experimental data taken at higher temperatures. The adjustable parameters,  $\beta_\alpha \equiv 1 - n_\alpha$ , and  $\tau_\alpha^*$ , are determined in the process. The results for  $\tau_\alpha^*$  and  $\beta_\alpha$  are shown in Table 2. The stretch exponent,  $\beta_\alpha$ , determined from the shear creep data has a slight temperature dependence. It starts out with the value of 0.50 at the higher temperature end and decreases with decreasing temperature down to about 0.44. The value of 0.50 is in agreement with the result of an independent dynamic mechanical measurement [22] of the shear modulus of two PMPS samples with molecular weights 12 000 and 130 000. These dynamic mechanical measurements were made in the relaxation frequency range corresponding to the retardation times of the creep measurements at which  $\beta_\alpha$  assumes the value of 0.50. Thus, there is

Table 2. Relaxation time,  $\tau_\alpha^*$ , and stretch exponent,  $\beta_\alpha$ , of the local segmental motion deduced from analysis of the recoverable creep compliance measurements.

T(C)	$\tau_\alpha^*$ (s)	$\beta_\alpha$
-50	$2.3 \times 10^5$	0.44
-46.9	$2.1 \times 10^3$	0.48
-45.2	$2.48 \times 10^2$	0.48
-44.5	$4.82 \times 10$	0.49
-42.6	9.7	0.50
-41.1	1.3	0.50

excellent agreement between the values of  $\beta_\alpha$  obtained by these two measurements under the same condition. It is interesting that we find the ratio of the relaxed compliance to the unrelaxed compliance for the local segmental motion of the polymer PMPS, given by  $J_{e\alpha}/J_g$ , is slightly larger than that of glass forming small molecular liquids like trinitrophenylbenzene, Aroclor, and sucrose benzoate [23]. For PMPS, we find

$$J_{e\alpha}/J_g = 5.2, \quad (7)$$

which can be compared with the value of about  $5 \gtrsim J_{e\alpha}/J_g \gtrsim 3$  for these small molecule liquids.

Next we examine the temperature dependence of the retardation time of the Rouse spectrum defined by  $\tau_{\max}$  at which  $L(\log \tau)$ , as shown in Fig. (3), assumes the maximum value. Another retardation time of the Rouse spectrum, not identical but closely related to  $\tau_{\max}$ , is the product  $\eta J_e^0$  of the viscosity and the steady state recoverable compliance at the same temperature. Both  $\tau_{\max}$  and  $\eta J_e^0$  are characteristic retardation times of the spectrum of Rouse modes. They can differ in magnitude but should have the same temperature dependence. From the experimental data of  $\eta$  and  $J_e^0$  (see Table 1) we calculate  $\eta J_e^0$  and compare with  $\tau_{\max}$  for different temperatures. These two relaxation times differ by approximately one order of magnitude, with  $\tau_{\max}$  being longer and they have the same temperature dependence as expected. In Fig. 5 we have plotted  $\log_{10} \tau_{\max}$  and  $\log_{10} (\eta J_e^0)$  as a function of temperature, adding a constant 1.25 to the  $\log_{10} (\eta J_e^0)$  data to shift them vertically upward and bring them to be nearly coincident with  $\log_{10} \tau_{\max}$ .

The relation between the various relaxation times are shown in Fig. 5. By inspection, we see that  $\tau_{\max}$  or  $\eta J_e^0$  of the Rouse modes and  $\tau_\alpha^*$  of the local segmental mode have very different temper-

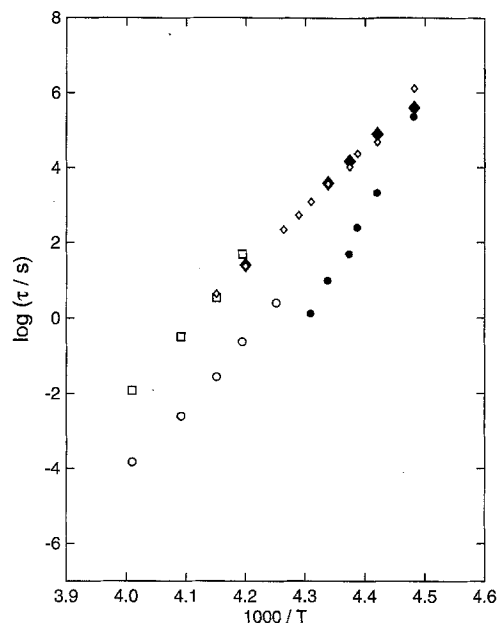


Fig. 5. Arrhenius plot of various relaxation times determined from the experimental data against  $1000/T$ . Filled circles denote  $\tau_\alpha^*$  determined from the fits in Fig. 4; filled diamonds denote  $\tau_{\max}$  determined from  $L$  shown the inset of Fig. 3; open diamonds denote  $\log_{10}$  of the products  $\eta J_e^0$ , shifted vertically upwards by 1.25 decades. Open circles denote  $\tau_f^*$  and open squares denote  $\tau_g^*$  from PCS measurements

ature dependences. As temperature is reduced, the separation in time scale between  $\tau_{\max}$  and  $\tau_\alpha^*$  decreases rapidly. This rapid decrease in separation between  $\tau_\alpha^*$  and  $\tau_{\max}$  leads to enroachment of the time scale of local segmental motion to that of the Rouse spectrum and causes the rapid decrease of the steady state recoverable compliance  $J_e^0$ . The mechanism based on time scale enroachment of the segmental motion towards the Rouse modes have been discussed in refs. [15] and [17]. It remain valid here as an explanation of the anomalous change of viscoelastic property with temperature observed in PMPS.

### III. Photon correlation spectroscopy measurements

#### a. Experimental section

The photon correlation spectroscopy (PCS) measurements were made at a scattering angle of  $\theta = 90^\circ$  in the temperature range 235.2

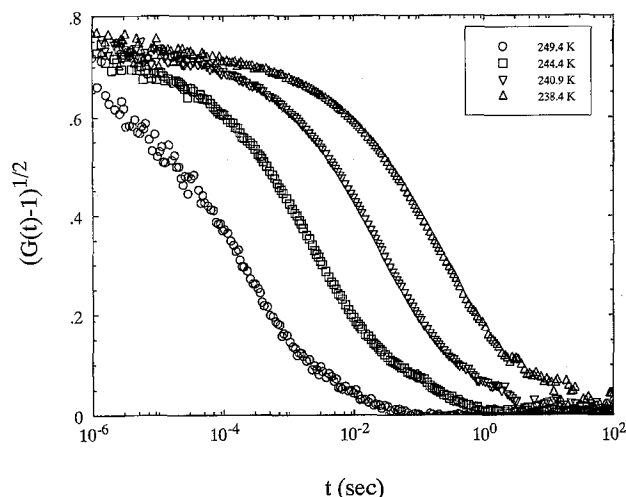


Fig. 6. Time correlation function from photon correlation spectroscopy measurement of PMPS at four temperatures

– 249.4 K. The light source was an Ar + laser (Spectra Physics, Model 2020) with a wavelength ( $\lambda$ ) of 488 nm and a stabilized power of 100 mW. The incident beam was polarized vertically (V) to the scattering plane by means of a Glan polarizer (Halle, Berlin) with extinction coefficient of  $10^{-6}$  and the scattered beam was polarized horizontally (H) by means of a Glan-Thompson analyzer with extinction coefficient of  $10^{-7}$ . Hence, the VH correlation functions were obtained in the range  $10^{-6} - 10^2$  s with the ALV-5000 multiple sampling time digital correlator. For homodyne conditions, the measured correlation function of scattered light intensity  $G(q, t)$  at a given scattering vector  $q (= 4\pi n/\lambda \sin(\theta/2))$ , where  $n$  is the refractive index) is related to the desired normalized time-correlation function  $g(q, t)$  by:

$$G(q, t) = A(1 + f|\alpha g(q, t)|^2), \quad (8)$$

where  $A$  is the base line measured at long times,  $f$  is the instrumental factor, and  $\alpha$  is the fraction of the total depolarized intensity associated with the fluctuations in the optical anisotropy of the material with dynamics longer than  $10^{-6}$  s. Figure 6 shows net correlation functions  $(G(q, t)/A - 1)^{1/2}$  of PMPS at four temperatures. It was worth noticing the high value of the short time intercept which justifies the use of homodyne conditions (Eq. (8)).

### b. Data analysis

The time-correlation functions (Fig. 6) were first fitted to a single Kohlrausch–Williams–Watts (KWW) decay function:

$$\sqrt{\frac{G(t)}{A} - 1} = b \exp[-(t/\tau^*)^\beta], \quad (9)$$

where  $b$ ,  $\tau^*$  and  $\beta$  are adjustable parameters. This fitting procedure produced systematic deviation plots especially at long times (Fig. 7a). Evidently, a “slow” process has to be included to fit the

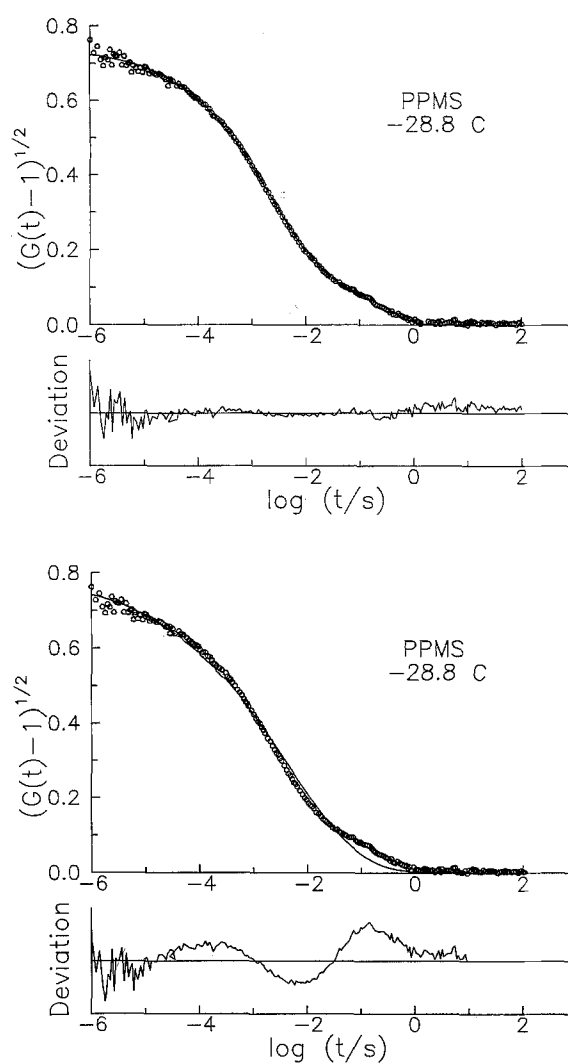


Fig. 7. Time correlation function from photon correlation spectroscopy measurements of PMPS at  $-28.8^\circ\text{C}$ : a) fitted to a single fast process (Eq. (9)) showing systematic deviation at long times; b) fitted to the sum of a fast and a slow process (Eq. (10)) with reduced deviation

Table 3. Amplitude, relaxation times and distribution of relaxation times of the PCS data (Eq. (10)).

T(K)	$b_f$	$\tau_f^*$ (s)	$\beta_f$	$b_s$	$\tau_s^*$ (s)
249.4	0.612	$1.47 \times 10^{-4}$	0.44	0.1	$1.2 \times 10^{-2}$
244.4	0.651	$2.457 \times 10^{-3}$	0.437	0.094	0.326
240.9	0.664	$2.767 \times 10^{-2}$	0.44	0.083	3.44
238.4	0.673	0.2363	0.421	0.07	48.6
235.2	0.651	2.539	0.451	—	—

correlation functions in addition to the “fast” KWW process:

$$\sqrt{\frac{G(t)}{A}} - 1 = b_f \exp[-(t/\tau_f^*)^{\beta_f}] + b_s \exp[-(t/\tau_s^*)], \quad (10)$$

which provides a good fit to the experimental data (Fig. 7b). In Eq. (10),  $b_f$  and  $b_s$  are the amplitude factors for the “fast” and “slow” processes,  $\tau_f^*$  and  $\tau_s^*$  are the corresponding relaxation times and  $\beta_f$  is the stretch exponent for the “fast” process. The parameters of Eq. (10) are summarized in Table 3.

### c. Results and discussion

Two processes have been observed in the depolarized PCS measurements. The “fast” process displays all the characteristics of the local segmental ( $\alpha$  -) relaxation. The amplitude ( $b_f$ ) is

nearly constant within the temperature range studied (Fig. 8) and so is the stretch exponent  $\beta_f$  which is equal to  $0.44 \pm 0.22$ . This value for  $\beta_f$  is in good agreement with the one determined by PCS and reported previously for a PMPS sample with a smaller molecular weight (MW = 2500)<sup>16</sup>. However,  $\beta_f$  is significantly smaller than  $\beta_\alpha$  determined from creep data, a conclusion readily obtained by comparing Tables 2 and 3. On the other hand, the “slow” process has a  $T$ -dependent amplitude (Fig. 8) and a narrow spectrum of retardation times which, within the experimental accuracy, is indistinguishable from a Debye process ( $\beta = 1$ ) although the uncertainty in the data can admit fits with  $\beta_f < 1$ . The amplitude of this process decreases with decreasing temperature (Table 3) and this is displayed in Fig. 8. This “slow” PCS process is not related to the long-range density fluctuations which have been observed [24] in some glass-forming liquids and polymers with polarized (VV) light scattering, for two reasons. first, this process is detected here in the VH-geometry and second the separation from the faster segmental process is about 1.9 decades in time only. Unambiguous identification of the “slow” PCS process based on the experimental data from a single MW sample is not possible. However, PCS measurements on a higher molecular weight PMPS sample (MW = 28 500) revealed again two modes in the polarized (VV) geometry [25]. At 16 K above  $T_g$ , the logarithmic difference of the retardation times was  $\sim 3.4$  decades. In comparison, at our highest measurement temperature ( $T - T_g \approx 8$  K) the logarithmic difference of the “slow” and “fast” processes is  $\sim 1.9$  decades (Table 3). Therefore, the “slow” mode in the high MW sample is 32 times slower as compared in the small MW sample and this coincides with the ratio of the squares of the two molecular weights. The  $M^2$ -dependence of  $\tau_s$  indicates that the “slow” process is related to the Rouse dynamics.

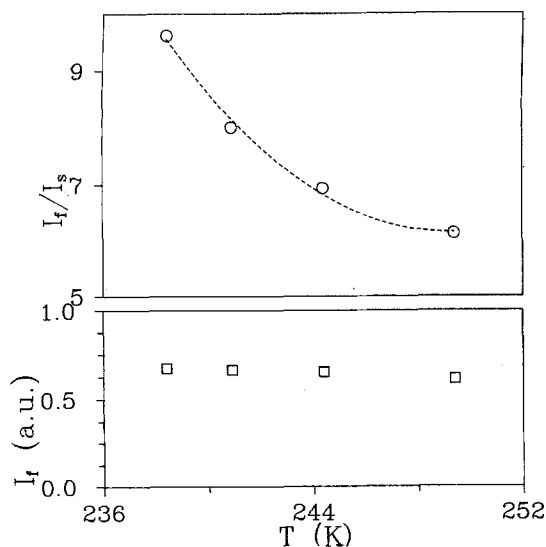


Fig. 8. Plot of  $I_f$  or equivalently  $b_f$  against temperature (lower). Plot of the ratio  $I_f/I_s$  or equivalently  $b_f/b_s$  against temperature (upper)

Having identified the origins of the “fast” and the “slow” processes with the local segmental relaxation and the Rouse dynamics respectively, we shall relate the decrease of the amplitude,  $b_s/b_f$ , of the slow process (Fig. 8) to the decrease of  $J_e^0$  observed by creep compliance measurement with decreasing temperature. Let us first make a comparison between the variations of  $b_s/b_f$  and  $J_e^0$  with temperature in Fig. 2. This figure shows that they have approximately the same temperature dependence in a temperature range common to PCS and creep compliance measurements. The good correspondence between their temperature dependences indicate that  $b_s/b_f$  and  $J_e^0$  provide similar information on the Rouse dynamics from two different kinds of measurements. Thus, PCS experiment in PMPS has also observed the anomalous temperature dependence of the Rouse dynamics seen first by recoverable creep compliance measurements. However, within the comparatively shorter time window and the corresponding higher temperature range of PCS measurement, the temperature variation of  $J_e^0$  becomes mild and  $J_e^0$  tends to level off to the value as predicted by the Rouse model.

The retardation times,  $\tau_f^*$  and  $\tau_s^*$ , are plotted in Fig. 5 to compare with the data from creep measurement. The gap between  $\tau_f^*$  and  $\tau_s^*$  which appears in Fig. 5 at the interface between the temperature ranges of PCS and creep measurement indicates that these two techniques are not monitoring identical dynamics. This is perhaps not totally surprising because depolarized PCS does not measure the shear compliance as creep does. The retardation time  $\tau_s^*$  seems to be longer than  $\tau_f^*$  by an order of magnitude at a common temperature in the interface region. Had we interpreted  $\tau_f^*$  as a relaxation time, then the discrepancy would be even worse because the corresponding retardation time is related [26] to the relaxation time by the factor  $J_{e\alpha}/J_g$ , which is about 5. This difference between  $\tau_f^*$  and  $\tau_s^*$  is accompanied by a corresponding difference between  $\beta_f$  and  $\beta_s$ , with  $\beta_f$  being smaller. In the coupling model [27] two different dynamic variables (longitudinal and shear compliances here) having different stretch exponents will have different retardation times. The dynamic variable having the smaller stretch exponent will have the longer retardation time, in accordance with the data presented here. On the other hand, the retar-

dation times for the Rouse spectrum determined by the two techniques,  $\tau_s^*$  and  $\tau_{\max}$ , are nearly the same (see Fig. 5). This fact is also consistent with the coupling model because for the Rouse modes the coupling parameter,  $n$ , is identically zero and hence the retardation times  $\tau_f^*$  and  $\tau_{\max}$  are the same for both dynamic variables.

Creep measurement shows that  $\tau_s^*$  has a much stronger temperature dependence than  $\tau_{\max}$  which leads to the rapid decrease of  $J_e^0$  with falling temperature, as discussed. In the explanation given in ref. [17] (see Eqs. (13, 14, 18) therein), these two effect are linked to each other in the sense that their degrees are proportional to each other. As we have shown in Fig. 2, in the temperature range of PCS measurements  $J_e^0$  has started to level off to the Rouse value. Hence,  $J_e^0$  exhibits only a mild decrease with decreasing temperature. Thus, we expect correspondingly the temperature dependence of  $\tau_f^*$  to be only slightly stronger than that of  $\tau_s^*$  from PCS measurement, which is indeed observed (see Fig. 5).

#### IV. Summary and conclusions

Although there was little doubt that the anomalous temperature dependent viscoelastic properties observed in low molecular weight poly(styrene) is a general phenomenon, until now experimental measurements on another polymer were not available to confirm this. The availability of low molecular weight poly(methylphenylsiloxane) with a narrow molecular weight distribution has made it worthwhile for us to repeat the shear creep and recoverable creep compliance,  $J_r(t)$ , measurements previously performed on PS. These results are qualitatively similar to that of PS. There is a dramatic breakdown of thermorheological simplicity reflected by a larger reduction of the recoverable creep compliance,  $J_e^0$ , with decreasing temperature. The local segmental contribution to the recoverable compliance has been isolated from the data and its effective retardation time is found to have a stronger temperature dependence than that of the Rouse spectrum. The coupling parameter,  $n_\alpha$ , of the local segmental motion for PMPS is temperature dependent, ranging from 0.50 to 0.58 and slightly smaller than that of PS, comparable to that of PVAc, and larger than that of poly(isobutylene)



[17]. According to the theory previously given [17], the anomalous viscoelastic behavior observed in low molecular weight PMPS is due to its having a sizeable  $n_z$  which in turn is responsible for the breakdown in thermorheological simplicity. All these features are confirmed by the results of an analysis of the recoverable creep compliance data. Photon correlation spectroscopy measurements under isothermal conditions have also been able to observe the local segmental motion and the Rouse dynamics within the time window available to this technique. The coupling parameter of local segmental motion deduced from PCS is slightly larger than that obtained from  $J_r(t)$ . An anomalous decrease of the amplitude of the time correlation function of the Rouse dynamics with decreasing temperature is remarkably similar to the decrease of  $J_e^0$  with decreasing temperature observed in the same temperature region by recoverable creep measurements. Thus, we may conclude that both recoverable shear creep compliance measurement and dynamic light scattering (i.e., PCS) have revealed the anomalous viscoelastic properties of PMPS as seen before in PS, which may indeed be general for low molecular weight polymers near their glass temperatures.

#### Acknowledgement

KLN is supported in part by ONR Contract N0001494WX23010.

#### References

1. Ferry JD (1980) *Viscoelastic Properties of Polymers*. 3rd ed. Wiley, New York
2. Plazek DJ (1965) *J Phys Chem* 69:3480; *J Polym Sci A2* 1968 6 621
3. Gray R, Harrison G, Lamb J (1976) *J Polym Sci Polym Phys Ed* 14:1361; *Proc. R. Soc London* 1977, 356, 77
4. Plazek DJ (1982) *J Polym Sci, Polym Phys Ed* 20:729
5. Plazek DJ (1980) *Poly J* 12:43
6. Plazek DL, Plazek DJ (1983) *Macromolecules* 16:1469
7. Fytas G, Floudas G, Ngai KL (1990) *Macromolecules* 23:1104
8. Alegria A, Macho E, Colmenero J (1991) *Macromolecules* 24:5196
9. Colmenero J (1991) *J Non-Cryst Solids* 131–133:860
10. Ngai KL, Plazek DJ (1986) *J Polym Sci Part B: Polym Phys Ed* 24:619
11. Ngai KL, Plazek DJ (1985) *J Polym Sci Polym Phys Ed* 23, 2159
12. Plazek DJ, Rosner MJ, Plazek DL (1988) *J Polym Sci: Part B: Polym Phys Ed* 26:473
13. Williams M, Ferry JD (1955) *J Colloid Sci* 10:474
14. Plazek DJ, O'Rourke J (1971) *J Polym Sci A2* 9:209
15. Ngai KL, Plazek DJ, Deo SS (1987) *Macromolecules* 20:3047
16. Ngai KL, Fytas G (1986) *J Polym Sci Polym Phys Ed* 24:1683; Fytas G, Dorfmueller Th, Chu B (1984) *J Polym Phys Ed* 22:1471
17. Ngai KL, Plazek DJ, C Bero (1993) *Macromolecules* 26:1065
18. Cochrane J, Harrison G, Lamb J, Phillips DW (1980) *Polymer* 21:837
19. Ngai KL, Schlosser E, Schönhals A (1992) *Macromolecules* 25:4915
20. Dean GD, Read BE, Tomlins PE (1990) *Plastic Rubber Process Appl* 13:37
21. Plazek DJ, Ngai KL (1991) *Macromolecules* 24:1222
22. Roland CM, Santangelo PG, Ngai KL, Meier G (1993) *Macromolecules* 26:6164
23. Plazek DJ (1991) *J Non-Cryst Solids* 131–133:836
24. Fischer EW, Meier G, Rabenau T, Patkowski A, Steffen W, Thönnies W (1991) *J Non-Cryst Solids* 131–133:134
25. Boese D, Momper B, Meier G, Kremer F, Hagenah J.-U, Fischer EW (1989) *Macromolecules* 22:4416
26. McCrum NG, Read BE, Williams G (1967) *Anelastic and Dielectric Effects in Polymeric Solids*. John Wiley & Sons, London
27. Ngai KL in "Disorder Effects in Relaxation Processes", Richard, R.; Blumen, A. (eds), Springer-Verlag, Heidelberg, 1994

Received May 10, 1994;  
accepted June 16, 1994

Authors' address:

D. J. Plazek  
Dept. of Materials Science and Engineering  
University of Pittsburgh  
Pittsburgh, PA 15261, USA